Biochemical Pharmacology 82 (2011) 1619–1629

Contents lists available at SciVerse ScienceDirect

Biochemical Pharmacology

journal homepage: www.elsevier.com/locate/biochempharm

Increased apoptotic efficacy of lonidamine plus arsenic trioxide combination in human leukemia cells. Reactive oxygen species generation and defensive protein kinase (MEK/ERK, Akt/mTOR) modulation

Eva Calviño [a,1], María Cristina Estañ [a,1], Gloria P. Simón [a], Pilar Sancho [b], María del Carmen Boyano-Adánez [b], Elena de Blas [a], Jacqueline Bréard [c], Patricio Aller [a,*]

[a] Centro de Investigaciones Biológicas, Consejo Superior de Investigaciones Científicas, Madrid, Spain
[b] Departamento de Bioquímica y Biología Molecular, Facultad de Medicina, Universidad de Alcalá, Alcalá de Henares, Madrid, Spain
[c] Institut National de la Santé et de la Recherche Médical, Hôpital Paul Brousse,Villejuif, France

ARTICLE INFO

Article history:
Received 4 May 2011
Accepted 22 August 2011
Available online 27 August 2011

Keywords:
Lonidamine
Arsenic trioxide
Apoptosis
ROS
Protein kinases

ABSTRACT

Lonidamine is a safe, clinically useful anti-tumor drug, but its efficacy is generally low when used in monotherapy. We here demonstrate that lonidamine efficaciously cooperates with the anti-leukemic agent arsenic trioxide (ATO, Trisenox™) to induce apoptosis in HL-60 and other human leukemia cell lines, with low toxicity in non-tumor peripheral blood lymphocytes. Apoptosis induction by lonidamine/ATO involves mitochondrial dysfunction, as indicated by early mitochondrial permeability transition pore opening and late mitochondrial transmembrane potential dissipation, as well as activation of the intrinsic apoptotic pathway, as indicated by Bcl-X_L and Mcl-1 down-regulation, Bax translocation to mitochondria, cytochrome *c* and Omi/HtrA2 release to the cytosol, XIAP down-regulation, and caspase-9 and -3 cleavage/activation, with secondary (Bcl-2-inhibitable) activation of the caspase-8/Bid axis. Lonidamine stimulates reactive oxygen species production, and lonidamine/ATO toxicity is attenuated by antioxidants. Lonidamine/ATO stimulates JNK phosphorylation/activation, and apoptosis is attenuated by the JNK inhibitor SP600125. In addition, lonidamine elicits ERK and Akt/mTOR pathway activation, as indicated by increased ERK, Akt, p70S6K and rpS6 phosphorylation, and these effects are reduced by co-treatment with ATO. Importantly, co-treatment with MEK/ERK inhibitor (U0126) and PI3K/Akt (LY294002) or mTOR (rapamycin) inhibitors, instead of ATO, also potentiates lonidamine-provoked apoptosis. These results indicate that: (i) lonidamine efficacy is restrained by drug-provoked activation of MEK/ERK and Akt/mTOR defensive pathways, which therefore represent potential therapeutic targets. (ii) Co-treatment with ATO efficaciously potentiates lonidamine toxicity via defensive pathway inhibition and JNK activation. And (iii) conversely, the pro-oxidant action of lonidamine potentiates the apoptotic efficacy of ATO as an anti-leukemic agent.

1. Introduction

Lonidamine (1-(2,4-dichlorobenzyl)-1H-indazole-3-carboxylic acid) was initially used as anti-spermatogenic agent, but its potential anti-tumor properties were also soon recognized. Lonidamine is a safe and well-tolerated drug, but having as a major limitation the poor clinical efficacy when used alone. Nevertheless, it proved to be an efficacious sensitizing agent when

Abbreviations: Akt/mTOR, protein kinase B/mammalian target of rapamycin; ANT, adenine nucleotide translocator; AML, acute myeloid leukemia; APL, acute promyelocytic leukemia; ATO, arsenic trioxide; CsA, cyclosporin A; DAPI, 4,6-diamino-2-phenylindole; DHE, dihydroethidium; DHR, dihydrorhodamine-123; H_2DCFDA, dichlorodihydrofluorescein diacetate; IL2, interleukin-2; IMP, inner mitochondrial membrane permeabilization; JNK, c-Jun NH_2-terminal kinase; LY294002, 2-(4-morpholinyl)-8-phenyl-4H-1-benzopyran-4-one; mAb, monoclonal antibody; MAPK, mitogen-activated protein kinase; MEK/ERK, mitogen-induced extracellular kinase/extracellular signal-regulated kinase; mPTP, mitochondrial transition pore; MTT, 3[4,5-dimethyl-2-thiazolyl]-2,5diphenyl-2H-tetrazolium bromide; NAC, *N*-acetyl-L-cysteine; pAb, polyclonal antibody; PBS, phosphate buffered saline; PBLs, peripheral blood lymphocytes; PEG–catalase, catalase–polyethylene glycol; PI3K, phosphatidylinositol 3-kinase; PHA, phytohemagglutinin; PI, propidium iodide; R123, rhodamine 123; ROS, reactive oxygen species; SP600125, anthra[1,9-*cd*]pyrazol-6(2*H*)-one; U0126, 1,4-diamino-2,3-dicyano-1,4-*bis*(2-aminophenylthio)butadiene; z-VAD-fmk, Z-Val–Ala–Asp(OMe)–CH_2F.

* Corresponding author at: Centro de Investigaciones Biológicas, CSIC, Ramiro de Maeztu 9, 28040 Madrid, Spain. Tel.: +34 918373112x4247/4248; fax: +34 91 5360432.
E-mail addresses: eva.calvino@cib.csic.es (E. Calviño), mcri.estan@cib.csic.es (M.C. Estañ), gloriapilar@cib.csic.es (G.P. Simón), pilar.sancho@uah.es (P. Sancho), carmen.boyano@uah.es (M.d.C. Boyano-Adánez), elena@cib.csic.es (E. de Blas), Jacqueline.breard@psud.fr (J. Bréard), aller@cib.csic.es (P. Aller).

[1] These authors equally contributed to this work.

0006-2952/$ – see front matter © 2011 Elsevier Inc. All rights reserved.
doi:10.1016/j.bcp.2011.08.017

combined with DNA-damaging chemotherapeutic treatments, such as radiation, alkylating drugs and anthracyclines [1]. Since lonidamine is an energolytic agent, it was hypothesized that inhibition of energy production might interfere with the repair mechanisms of DNA damage produced by the genotoxic treatments. In combined therapies, the clinical value of lonidamine was clearly proved in phase II and III assays against a variety of solid tumors [1], although a potential application in leukemic diseases was also insinuated in *in vitro* pre-clinical assays [2,3]. Lonidamine was characterized as a mitochondria-targeting drug capable of binding the adenine nucleotide translocator (ANT), causing mitochondrial permeability transition pore (mPTP) opening and apoptosis [4]. Other reported biochemical effects, also important for cell death, are inhibition of mitochondria-bound hexokinase, which decreases glycolytic activity and intracellular ATP levels; inhibition of mitochondrial respiration; inhibition of lactate efflux from the cell, causing intracellular acidification; and inhibition of drug extrusion mechanisms, reversing the multi-drug resistance phenotype [1]. However, the effects of lonidamine on protein kinase activities and other signaling mechanisms, important to understand cell death regulation and eventually improve drug efficacy, are largely unknown.

Arsenic trioxide (ATO, Trisenox™) is a recently established, clinically efficacious agent for the treatment of acute promyelocytic leukemia (APL) [5,6]. At low, physiologically tolerable concentrations this agent promotes terminal cell differentiation of APL cells, an effect likely derived from the destruction of the promyelocytic leukemia–retinoic acid receptor α (PML-RARα) fusion onco-protein, characteristic of this disease. However, it exhibits other multiple biochemical and molecular mechanisms. Thus, as in the case of lonidamine, ATO binds ANT leading to mPTP opening and apoptosis [4]. In addition, it stimulates ROS over-production, either from mitochondrial or extra-mitochondrial sources; elicits death-receptor (DR5, TNF-R1) over-expression; causes cytoskeleton and mitotic spindle disruption; and alters protein kinase-mediated signaling pathways and transcription factors [5–7]. Because of this, ATO induces apoptosis in multiple tumor cell types and hence appears as a potentially useful agent against hematological malignancies and solid tumors, other than APL [7,8]. Nonetheless, the clinical application of ATO as single agent may be limited by the requirement of high toxic doses to effectively induce apoptosis. Hence, extending the therapeutic application of ATO would require the generation of sensitizing strategies, allowing decreasing the effective drug concentrations.

The facts that both lonidamine and ATO are mitochondria-targeting drugs with otherwise different action mechanisms, lead us to consider the possible benefits of combining these agents. As a first, pre-clinical approach, in the present work we examine the possible cooperation between lonidamine and ATO to reduce cell growth and induce apoptosis in HL-60 and other human leukemia cell lines, and investigate some essential biochemical and signaling mechanisms explaining such cooperation. The results indicate that the combination of lonidamine plus ATO, used at clinically attainable but in themselves poorly effective concentrations, efficaciously induce apoptosis in leukemia cells with little toxicity in non-tumor proliferating peripheral blood lymphocytes. Among other mechanisms possibly accounting for increased apoptosis, ATO may potentiate lonidamine toxicity by attenuating drug-provoked activation of mitogen-induced extracellular kinase/extracellular signal-regulated kinase (MEK/ERK) and protein kinase B/mammalian target of rapamycin (Akt/mTOR) defensive pathways, while lonidamine may potentiate ATO toxicity via generation of moderate oxidative stress.

2. Materials and methods

2.1. Reagents and antibodies

All components for cell culture were obtained from Invitrogen, Inc. (Carlsbad, CA). Dichlorodihydrofluorescein diacetate (H_2DCFDA) was obtained from Molecular Probes, Inc. (Eugene, OR). Dihydroethidium (DHE, supplied as a 5 mM solution in dimethyl sulfoxide) and MitoTracker® RED CMXRos were obtained from Invitrogen, Inc. 4,6-diamino-2-phenylindole (DAPI) was obtained from Serva (Heidelberg, Germany). Cyclosporin H was obtained from Santa Cruz Biotechnology, Inc. (Santa Cruz, CA). The kinase inhibitors 1,4-diamino-2,3-dicyano-1,4-*bis*(2-aminophenylthio)butadiene (U0126), 2-(4-morpholinyl)-8-phenyl-4H-1-benzopyran-4-one (LY294002), anthra[1,9-*cd*]pyrazol-6(2*H*)-one (SP600125) and rapamycin, and the caspase inhibitor Z-Val–Ala–Asp(OMe)–CH_2F (z-VAD-fmk), were obtained from Calbiochem (Darmstad, Germany). Rabbit anti-human p38-MAPK, phospho-p38-MAPK (Thr^{180}/Tyr^{182}), SAPK/JNK, p44/42 MAPK, phospho-p44/p42 MAPK (Thr^{202}/Tyr^{204}), Akt, phospho-Akt (Ser^{473}), phospho-S6 ribosomal protein ($Ser^{235/236}$) (rpS6), HtrA2, and caspase-3 polyclonal antibodies (pAbs), and mouse anti-human phospho-p70 S6 kinase (Thr^{389}) (1A5) (p70S6K) and anti-caspase-8 (1C12) monoclonal antibodies (mAbs), were obtained from Cell Signaling Technology Inc. (Danvers, MA). Anti-ACTIVE® JNK pAb, Rabbit, (pTPpY) was obtained from Promega Corporation (Madison, WI). Mouse anti-pigeon cytochrome *c* mAb clone 7H8.2C12 was obtained from BD PharMingen (San Diego, CA). Mouse anti-human Bcl-2 (100) and prohibitin (6K2D1) mAbs; rabbit anti-human Bax (N-20), Bcl-$x_{S/L}$(S-18), Mcl-1(s-19) and caspase-9 p35 (H-170) pAbs; and goat anti-human Bid (C-20) and HHK II (C-14) pAbs were from Santa Cruz Biotechnology, Inc. Mouse anti-XIAP (clone 2F1) mAb was obtained from MBL International Corporation (Woburn, MA). Mouse anti-OxPhos Complex IV subunit I (anti-cytochrome oxidase subunit I, COX I) mAb was obtained from Molecular Probes, Inc. Peroxidase-conjugated immunoglobulin G antibodies were obtained from DAKO Diagnostics, S.A. (Barcelona, Spain). All other non-mentioned reagents and antibodies were from Sigma (Madrid, Spain).

2.2. Cells and treatments

The human leukemia cell lines HL-60 and U937 (acute myeloid leukemia, AML), NB4 (acute promyelocytic leukemia, APL), and RPMI 8866 (B lymphoblastic leukemia), and stably Bcl-2-transfected U937 cells (U4 clone) [9], were routinely grown in RPMI 1640 supplemented with 10% (v/v) heat-inactivated calf serum, 0.2% sodium bicarbonate and antibiotics in a humidified 5% CO_2 atmosphere at 37 °C. Experiments were carried out at the logarithmic growth phase (approximate cell concentration at the initiation of experiments: 2×10^5 cells/ml for 16–24 h treatments, and 4×10^5 cells/ml for 3–6 h treatments). Human peripheral blood lymphocytes (PBLs) were isolated from buffy coats from healthy donors over a Lymphoprep (Nycomed, Norway) gradient according to standard procedures. The lymphocytes were re-suspended at $0.5–1 \times 10^6$ cells/ml in RPMI 1640 plus 10% (v/v) heat-inactivated calf serum, and stimulated to proliferate for 2 days with 1 μg/ml phytohemagglutinin (PHA), followed by 5 days incubation with 20 U/ml of human interleukin-2 (IL-2) before initiation of the treatments. Under these conditions the PBLs exhibited an approximate doubling time of 24 h.

Calcein-AM was commercially obtained as a 4 mM solution in dimethyl sulfoxide. Stock solutions of H_2DCFDA (3 M), cyclosporin A (CsA), U0126, LY294002 and SP600125 (20 mM each), z-VAD-fmk (25 mM), lonidamine (100 mM), *N*-acetyl-L-cysteine (NAC, 3 M), and rapamycin (10 mM) were prepared in dimethyl sulfoxide. Rhodamine 123 (R123, 1 mg/ml) and cyclosporin H (10 mM) were prepared

in ethanol. Catalase–polyethylene glycol (PEG–Cat) was dissolved in a mixture of distilled water/glycerol at 20,000 U/ml. A stock solution of dihydrorhodamine-123 (DHR, 20 mM) was prepared in distilled water. 3(4,5-Dimethyl-2-thiazolyl)-2,5diphenyl-2H-tetrazolium bromide (MTT) was dissolved at 5 mg/ml in phosphate buffered saline (PBS). All these solutions were stored at −20 °C. Stock solutions of DAPI (10 mg/ml), propidium iodide (PI, 1 mg/ml) and PHA (5 mg/ml) were prepared in PBS. IL-2 was dissolved in RPMI/calf serum at 10,000 U/ml. ATO was initially dissolved in a small amount of 1 N NaOH, and then diluted with PBS to give a final concentration of 10 mM. These solutions were stored at 4 °C. Verapamil was freshly prepared in distilled water at 10 mM just before application.

2.3. Flow cytometry

The analysis of samples was carried out using an EPICS XL flow cytometer (Coulter, Hialeah, FL) equipped with an air-cooled argon laser tuned to 488 nm. The specific fluorescence signals corresponding to H_2DCFDA, calceín-AM, R123 and DHR were collected with a 525-nm band pass filter, and the signals corresponding to DHE and PI with a 620-nm band pass filter. A total of 10^4 cells were scored in each assay.

2.4. Measurement of cell proliferation and viability, cell cycle, apoptosis and necrosis

Cell proliferation was determined by total cell counting, using a TC10™ Automated Cell Counter, Bio-Rad Laboratories, S.A. (Madrid, Spain). Cell viability was determined by the MTT colorimetric assay, as previously described [10]. Cell cycle phase distribution was determined by cell permeabilization followed by PI staining and flow cytometry analysis. This technique also provided an estimation of the frequency of apoptotic cells, characterized by low (sub-G_1) DNA content. In addition, apoptosis was characterized by chromatin condensation/fragmentation, as determined by cell permeabilization followed by DAPI staining and microscopy examination. Finally, the criterion for necrosis (either genuine, "primary" necrosis or apoptosis-derived, "secondary" necrosis) was the loss of plasma membrane integrity, as determined by free PI uptake into non-permeabilized cells and flow cytometry analysis. Detailed description of these techniques was presented in a preceding work [11], and hence is omitted here.

2.5. Determination of mitochondrial membrane permeabilization and transmembrane potential dissipation

Inner mitochondrial membrane permeabilization (IMP) was determined using the calcein-AM/$CoCl_2$ method reported by Petronilli et al. [12], with adaptations for flow cytometry [13] or spectrophotometry using HL-60 cells [14]. With this aim, the cells were collected by centrifugation, extensively washed with PBS, and incubated for 15 min at 37 °C in serum-and red phenol-free RPMI medium containing 1 μM calcein-AM and 1 mM $CoCl_2$. After medium removal the cells were extensively washed with PBS, re-suspended in the culture medium where originally grown, and subjected to the desired treatments. At the end of treatments the cells were placed on ice and rapidly analyzed by flow cytometry. Control assays using confocal microscopy corroborated the preferential labelling of mitochondria by calcein following this procedure (see Supplementary Figure 1). Mitochondrial transmembrane potential ($\Delta\Psi_m$) dissipation was determined using the cationic agent R123 and flow cytometry analysis, as earlier described [15].

2.6. Determination of ROS

The intracellular accumulation of ROS was determined using the fluorescent probes H_2DCFDA, DHE and DHR. H_2DCFDA is a general indicator of ROS production [16], while DHE and DHR preferentially measure anion superoxide and peroxides, respectively [17]. With this aim, at the end of treatments the cells were labelled (30 min at 37 °C) with the corresponding probe (5 μM), extensively washed with cold PBS, re-suspended in cold RPMI medium, and rapidly analyzed by flow cytometry. Internal controls using unlabelled cells indicated that lonidamine and ATO autofluorescence was null at all assayed conditions.

2.7. Cell fractionation and immunoblot assays

To obtain total cellular protein extracts, cells were collected by centrifugation, washed with PBS, and lysed for 20 min at 4 °C in a buffer consisting of 20 mM Tris–HCl, pH 7.5, containing 137 mM NaCl, 10% (v/v) glycerol and 1% (v/v) Nonidet P-40, supplemented with a commercial protease inhibitor cocktail, 1 mM sodium orthovanadate and 10 mM NaF. After centrifugation (10,000 × *g* for 15 min at 4 °C), the supernatants were collected. Cytosolic extracts, aimed at determining cytochrome *c* and Omi/HtrA2 release from mitochondria, were obtained by cell permeabilization with digitonin, following the previously described procedure [18]. The remaining membrane fraction was lysed with Laemmli's buffer and used as a mitochondria-enriched fraction to determine Bax translocation or cytochrome *c* remaining in mitochondria. Fractions of total, mitochondria-enriched or cytosolic extracts, containing equal protein amounts, were analyzed by SDS-polyacrylamide gel electrophoresis, blotted onto membranes, and immunodetected, as previously described [19].

2.8. Statistical analysis

As a rule, the results were expressed as mean value ± SD. When considered convenient, the significance of differences between experimental conditions was examined using the Student's *t*-test. Differences with $p < 0.05$ were considered as significant (*), and with $p > 0.05$ as non-significant (n.s.).

3. Results

3.1. Apoptosis induction

Fig. 1 shows the capacity of lonidamine and ATO to decrease cell growth and induce apoptosis in HL-60 cells. ATO was used at 2 μM, a clinically useful concentration [5] earlier selected as adequate for combined treatments in AML cell lines [10,18]. Treatment with ATO for 24 h slightly decreased cell proliferation, as determined by cell counting (Fig. 1A), but caused minimal apoptosis, as determined by chromatin condensation/fragmentation (Fig. 1B). Lonidamine was initially assayed at concentrations of 25–200 μM, demonstrating dose-dependent effects on both cell proliferation and apoptosis (Fig. 1A and B). At 50 and 100 μM – equivalent to 16 and 32 μg/ml, respectively, described as attainable concentrations in plasma [1] – apoptosis induction was negligible (50 μM) or low (100 μM). However, both general toxicity (measured by the MTT assay) and apoptosis were greatly increased when lonidamine was combined with ATO (Fig. 1B and C). Apoptosis execution was apparently null during the first 6 h of treatment, and started to be manifested at hour 16 in the combined treatments (Fig. 1D). Flow cytometry assays confirmed apoptosis potentiation by lonidamine plus ATO, measured by sub-G_1 DNA content (Fig. 1E). The flow cytometry profiles also indicated that ATO and lonidamine alone do not produce gross alterations in cell cycle distribution. However, in the lonidamine plus ATO treatment the relative reduction in the fraction of viable cells mainly affected the S and G_2/M subpopulations (Fig. 1E), suggesting either a higher sensitivity of these cycle phases to apoptosis, or some cell cycle

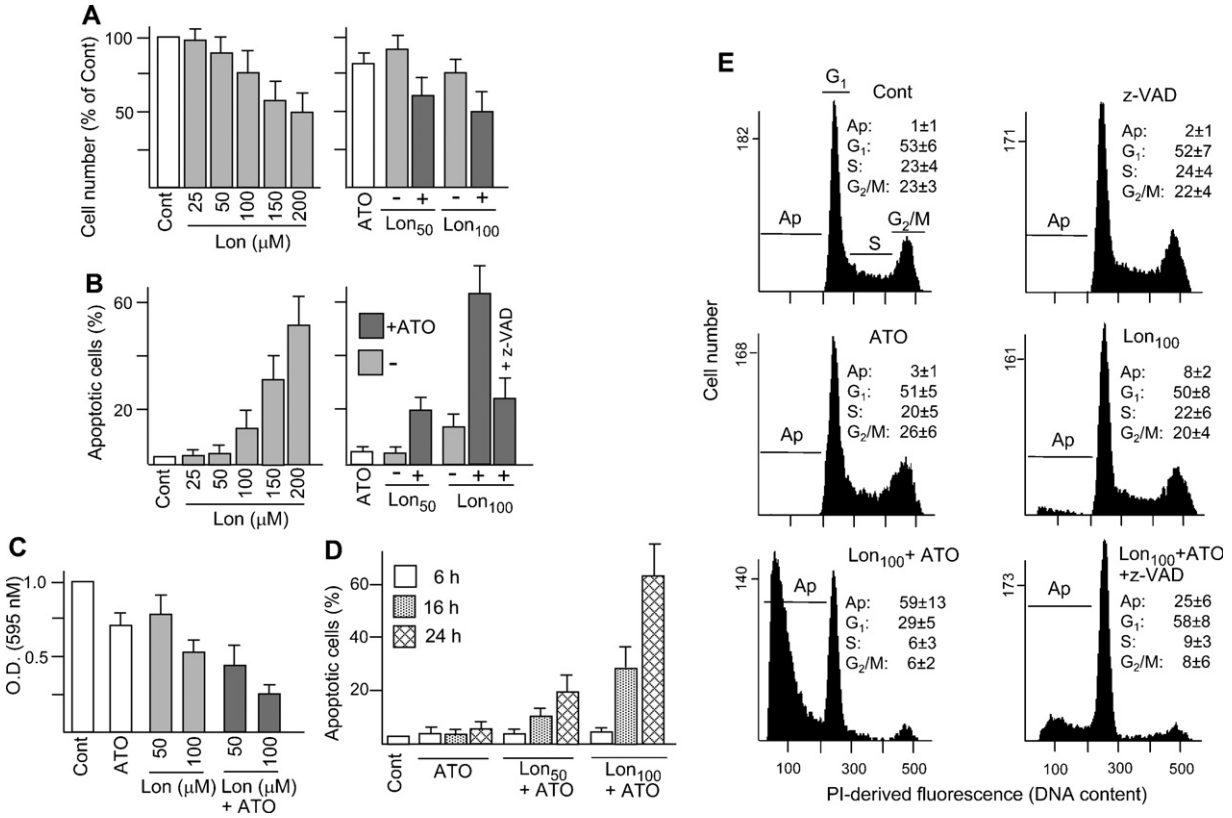

Fig. 1. Apoptosis induction and cell cycle effects caused by lonidamine and ATO in HL-60 cells. Cell cultures were either untreated (Cont) or treated for 24 h (A–C and E) or for the indicated time-periods (D) with 2 μM ATO or the indicated concentrations of lonidamine (Lon), alone or in combination. (A) Cell proliferation activity, as measured by total cell number counting. The results are expressed in relation to the control, which received the arbitrary value of 100 (approximate doubling time in controls, 18 h). (B and D) Frequency of apoptotic cells, as determined by chromatin condensation/fragmentation. Where indicated, the cells were pre-incubated for 30 min with the caspase inhibitor z-VAD-fmk (50 μM). (C) Changes in cell viability, as determined by the MTT assay. The absorption values are represented in relation to control, which received the arbitrary value of 1.0. (E) Cell cycle distribution according to DNA content. Cells with sub-G_1 DNA content are considered as apoptotic (Ap). Values in A–D represent the mean ± SD of at least three determinations. The flow cytometry profiles in (E) are representative of one of three determinations, and the values (representing percentages of cells in each cycle phase) indicate the mean ± SD of the three assays. For convenience, lonidamine concentrations (μM) are frequently represented as a subscript.

delay at G_1. Co-treatment with z-VAD-fmk considerably decreased ATO plus lonidamine provoked-apoptosis, confirming that the observed cell death is at least in part caspase-dependent apoptosis (Fig. 1B and E). Finally, a minor fraction of cells (about 15% above control values) exhibited free PI penetration at 24 h of treatment with 100 μM lonidamine plus ATO. Since this fraction was suppressed by co-treatment with z-VAD-fmk (results not shown), it likely represents "secondary" (late, apoptosis-derived) necrosis, rather then a genuine necrotic response.

The generation of apoptosis by lonidamine and ATO was also examined in other human leukemia cell lines, namely U937 (AML), NB4 (APL), and RPMI 8866 lymphoblastic cells. PHA/IL-2-stimulated PBLs obtained from healthy donors were used as a non-tumor cell model. The results are indicated in Fig. 2. Allowing for some quantitative differences in drug sensitivities, lonidamine and ATO cooperated with variable efficacy (but always in more than additive manner) to induce apoptosis in all leukemic cell lines. On the other hand, non-tumor PBLs were little affected by lonidamine and ATO, used alone or in combination. These results were qualitatively corroborated by flow cytometry (results not shown).

3.2. Mitochondria regulatory events

Once demonstrated the potentiation of apoptosis by lonidamine plus ATO, we wanted to analyze some biochemical mechanisms, which might explain the cooperative effect. Firstly, we focused the attention on mitochondria-related events, since as indicated above lonidamine and ATO are mitochondria-targeting drugs able to induce mPTP opening. This may include IMP and as a consequence $\Delta\Psi_m$ dissipation, as well outer membrane permeabilization (OMP) allowing the release of apoptosis-related soluble factors. For this reason, flow cytometry assays were carried out to measure early IMP using calcein-AM/$CoCl_2$, and late $\Delta\Psi_m$ dissipation using the cationic agent R123. Some of the obtained results are represented in Fig. 3. Lonidamine induced IMP, as revealed by the decrease in calcein-derived fluorescence (Fig. 3A). This was an early response (3 and 6 h), which preceded apoptosis execution. The lonidamine-provoked decrease in fluorescence was in part attenuated by co-treatment with 10 μM CsA, a mPTP inhibitor (Fig. 3A), while co-treatment with the inactive analog cyclosporin H (10 μM) was ineffective (not shown results). Nonetheless the results with CsA must be considered with caution, since this agent was toxic after prolonged exposure (not shown results), and may *per se* induce mPTP and apoptosis in leukemia cell models [[20], and references therein]. On the other hand, at the low concentration used (2 μM) ATO did not affect calcein-derived fluorescence, and what is it more important failed to potentiate lonidamine-provoked IMP, which clearly contrasts with the potentiation of apoptosis markers (see Fig. 1). Concerning $\Delta\Psi_m$, treatment for 16 and 24 h with lonidamine plus ATO caused the appearance of a discrete subpopulation of cells with low potential. This subpopulation was abrogated by z-VAD-fmk (upper curves in Fig. 3B, and other results not shown) and hence probably represents the fraction of cells undergoing apoptosis. In addition, treatments with lonidamine and ATO, alone and in combination, elicited a slight decrease in R123-derived fluorescence affecting the main (high $\Delta\Psi_m$) population, which, at least in the case of lonidamine plus ATO, was not prevented by z-VAD-fmk (Fig. 3B).

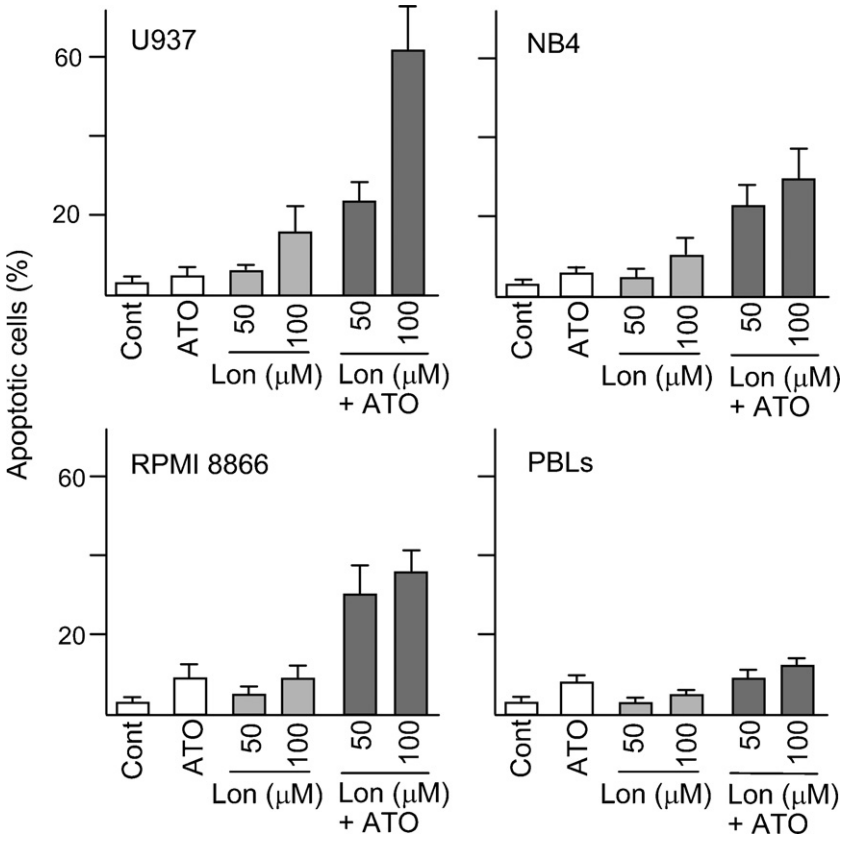

Fig. 2. Apoptosis induction in other cell types. The figure shows the frequency of apoptotic cells, measured by chromatin condensation/fragmentation, in U937, NB4 and RPMI 8866 human leukemia cells, and in PHA/IL2-stimulated PBLs, subjected for 24 h to the indicated treatments. ATO was used at 1 μM with NB4 and RPMI 8866 cells, and at 2 μM with U937 cells and PBLs. The results corresponding to PBLs represent mean ± SD of seven determinations with samples obtained from three different donors. All other conditions were as in Fig. 1.

Noteworthy, control experiments revealed that labelling with calcein-AM (without $CoCl_2$) or R123 was not affect by co-treatment with multidrug resistant (MDR) pump inhibitors such as verapamil or CsA (Supplementary Figure 2). This confirms the character of HL-60 as a MDR-negative cell line, and suggests that the here observed modifications in IMP (calcein-AM/$CoCl_2$) or $\Delta\Psi_m$ (R123) are not artifacts due to alterations in plasma membrane drug efflux activities.

Then, immunoblot assays were carried out to measure possible changes in expression and processing of proteins, which regulate the "intrinsic" (mitochondria-initiated) apoptotic pathway. This included anti-apoptotic (Bcl-2, Bcl-X_L, and Mcl-1) and pro-apoptotic (Bax) Bcl-2 family members, cytochrome *c* and Omi/HtrA2 mitochondria-localized proteins, the inhibitor of apoptosis protein (IAP) family member XIAP, and caspases-9 and -3 [21]. The results, obtained at 16 and 24 h are represented in Fig. 4A, and may be summarized as follows: (i) the treatments did not affect Bcl-2 expression (result not shown), but decreased Bcl-X_L and Mcl-1 expression. (ii) The treatments did not affect total Bax expression (result not shown), but stimulated its translocation to mitochondria, as demonstrated by the increase in mitochondria-enriched sub-cellular fraction and the decrease in cytosolic fraction. (iii) The treatments stimulated the release of cytochrome *c* and Omi/HtrA2 to cytosol, as demonstrated by the increase in cytosolic fraction, and in the case of cytochrome *c* also by the decrease in mitochondria-enriched fraction. Cytochrome *c* release is required for apoptosome assembly and activation, while the proteolytic action of Omi/HtrA2 is probably responsible for the here-observed down-regulation of XIAP, relieving caspases from the inhibitory action exerted by this protein. (iv) In fact, the treatments caused cleavage/activation of initiator caspase-9 as well as of effector caspase-3. (v) In addition to these canonic mitochondria-related events, the treatments caused caspase-8 cleavage/activation as well as slight truncation/activation of pro-apoptotic Bid, as indirectly manifested by the decrease in the amount of the 23 kDa Bid pro-form. In general, maximal alterations were produced by the combined (lonidamine plus ATO) treatment, which is consistent with the potentiation of apoptosis generation.

Caspase-8 and Bid activation is normally associated to the "extrinsic" (death receptor-initiated) apoptotic pathway [21]. Because of this, determinations were carried out using a Bcl-2-transfected U937 cell clone (U4), which exhibits an approximately 6- to 8-fold increase in Bcl-2 in comparison with normal U-937 cells (result not shown). As expected Bcl-2 over-expression inhibited the mitochondrial pathway, as indicated by the blockade of caspase-9 cleavage (Fig. 4B), and terminal apoptosis (Fig. 4C), but in addition prevented caspase-8 cleavage (Fig. 4B). This indicates that activation of the caspase-8/Bid axis by lonidamine plus ATO likely represents a secondary event derived from mitochondrial activation.

3.3. Oxidative stress

ATO is an oxidant-sensitive anti-tumor drug, the toxicity of which is dependent on the inherent intracellular ROS content [22] and potentiated by co-treatment with other pro-oxidant agents [18,23]. In addition, lonidamine was reported to inhibit electron transport in tumor cell mitochondria [24], which may in turn result in increased ROS production [23]. For these reasons, flow cytometry determinations using ROS-sensitive fluorescent probes were carried out to examine ROS production in lonidamine-treated HL-60 cells. Some of the obtained results are indicated in Fig. 5A.

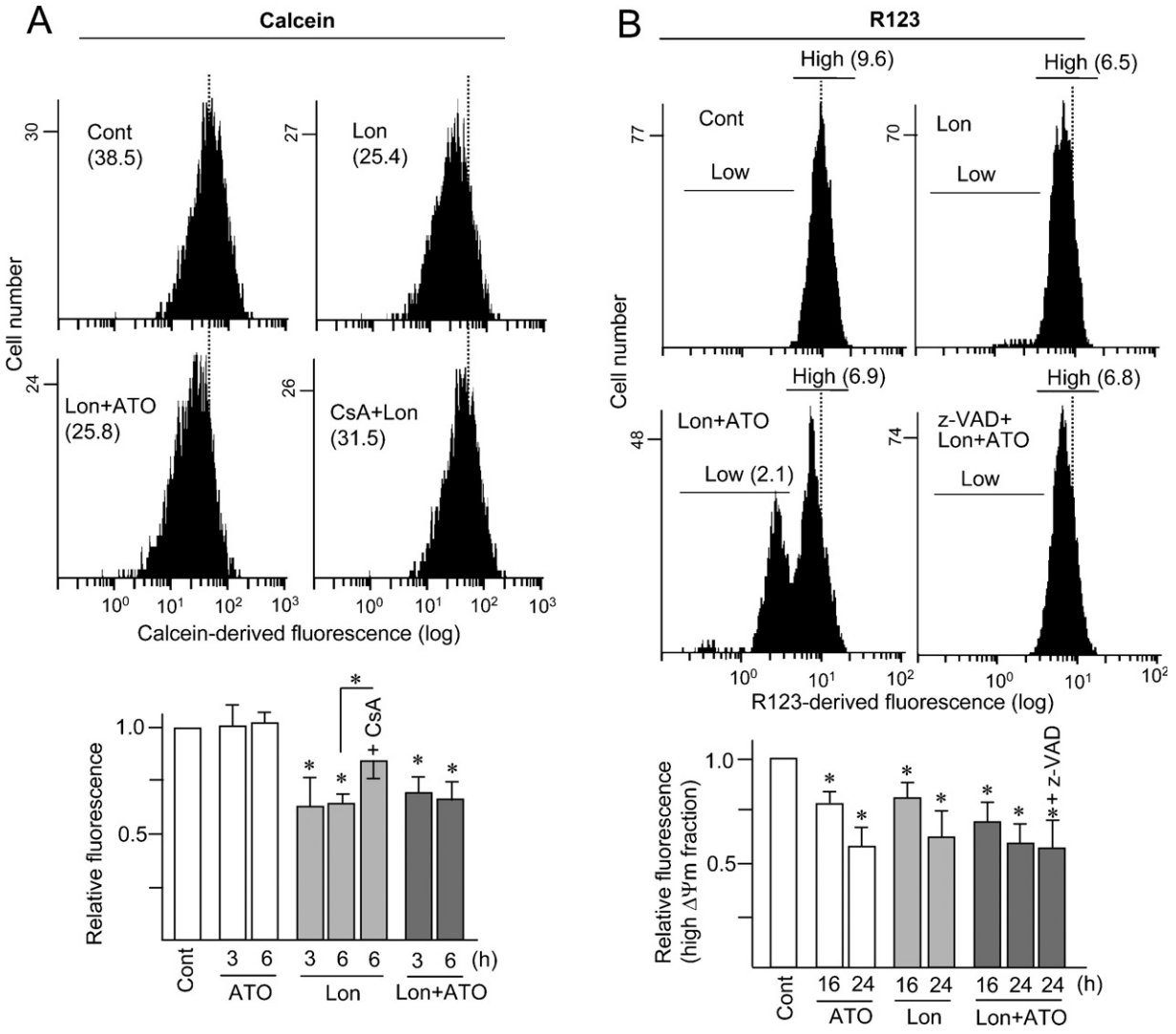

Fig. 3. Inner mitochondrial membrane permeabilization (IMP) and mitochondrial transmembrane potential ($\Delta\Psi_m$) dissipation. (A and B) HL-60 cells were treated for the indicated time-periods with 2 μM ATO and 100 μM lonidamine, alone or in combination. (A) The flow cytometry profiles show IMP generation, measured by loss of fluorescence in calcein-AM/$CoCl_2$ assays, at 6 h of treatment. The numbers into parenthesis indicate mean fluorescence values, as provided by the cytometer. The vertical dotted lines, corresponding to the mean fluorescence in the control, are represented in all profiles to better discern the displacement caused by the treatments. Cyclosporin A (CsA, 10 μM) was applied 30 min before the other drugs. The bar chart shows the results (mean ± SD) of at least four assays, represented in relation to controls, which received the arbitrary value of 1.0. (B) The flow cytometry profiles indicate $\Delta\Psi_m$ dissipation, measured by the loss of R123-derived fluorescence, at 24 h of treatment. Note the appearance of a subpopulation of cells with marked loss of fluorescence (low-$\Delta\Psi_m$) in the lonidamine plus ATO treatment, which is abrogated by pre-treatment with z-VAD-fmk. The numbers into parenthesis indicate mean fluorescence values for the high- and (when pertinent) the low-$\Delta\Psi_m$ subpopulations, as provided by the cytometer. The vertical dotted lines, corresponding to the mean fluorescence in the control, are represented in all profiles to better discern the displacement caused by the treatments. The bar chart indicates fluorescence values (mean ± SD) of at least three assays corresponding to the main peak (high-$\Delta\Psi_m$), expressed in relation to controls (arbitrary value of 1.0). Asterisks indicate significant differences in relation to control, or between the indicated pair of values. All other conditions were as in Fig. 1.

Treatment for 3 and 6 h with lonidamine, alone and with ATO, produced only slight increases in fluorescence using the peroxide-sensitive probe DHR, and using the anion superoxide-sensitive probe DHE in the case of lonidamine plus ATO. However a higher, dose-dependent response was obtained using H_2DCFDA, a highly sensitive non-specific probe which measures generalized oxidative stress [16]. Pre-treatment with PEG–catalase, a permeable form of the H_2O_2 scavenger catalase, attenuated the toxicity of lonidamine plus ATO, proving the importance of ROS over-production for apoptosis in the combined treatment (Fig. 5B). Pre-treatment with the antioxidant agent NAC (5–10 mM) attenuated apoptosis generation by 50 μM lonidamine plus ATO, but was ineffective or even increased the toxicity when lonidamine was used at 100 μM (results not shown). Noteworthy, PEG–catalase abrogated the late appearance of the low-$\Delta\Psi_m$ (z-VAD-fmk-inhibitable) subpopulation in lonidamine plus ATO-treated cells, but did not prevent the slight $\Delta\Psi_m$ decrease affecting the main (high-$\Delta\Psi_m$) subpopulation (Fig. 5C), or the decrease in fluorescence in calcein-AM/$CoCl_2$ assays (Fig. 5D).

As a complementary assay, we examined possible alterations in intracellular reduced glutathione (GSH) content, since ATO toxicity inversely correlates with GSH level. The results did not reveal significant alterations in GSH content, measured by monochlorobimane derivatization [15], after 24 h treatment with lonidamine, alone and in combination with ATO (results not shown).

3.4. Protein kinase modulation

Apoptosis generation is regulated by multiple protein kinases, among which ERKs and Akt usually play defensive, anti-apoptotic roles, while stress-activated protein kinase 1 (c-Jun NH_2-terminal kinase, JNK) and stress-activated protein kinase 2 (p38) may function as pro-apoptotic or defensive kinases [7,25,26]. Because of this, we analyzed the phosphorylation/activation of these kinases

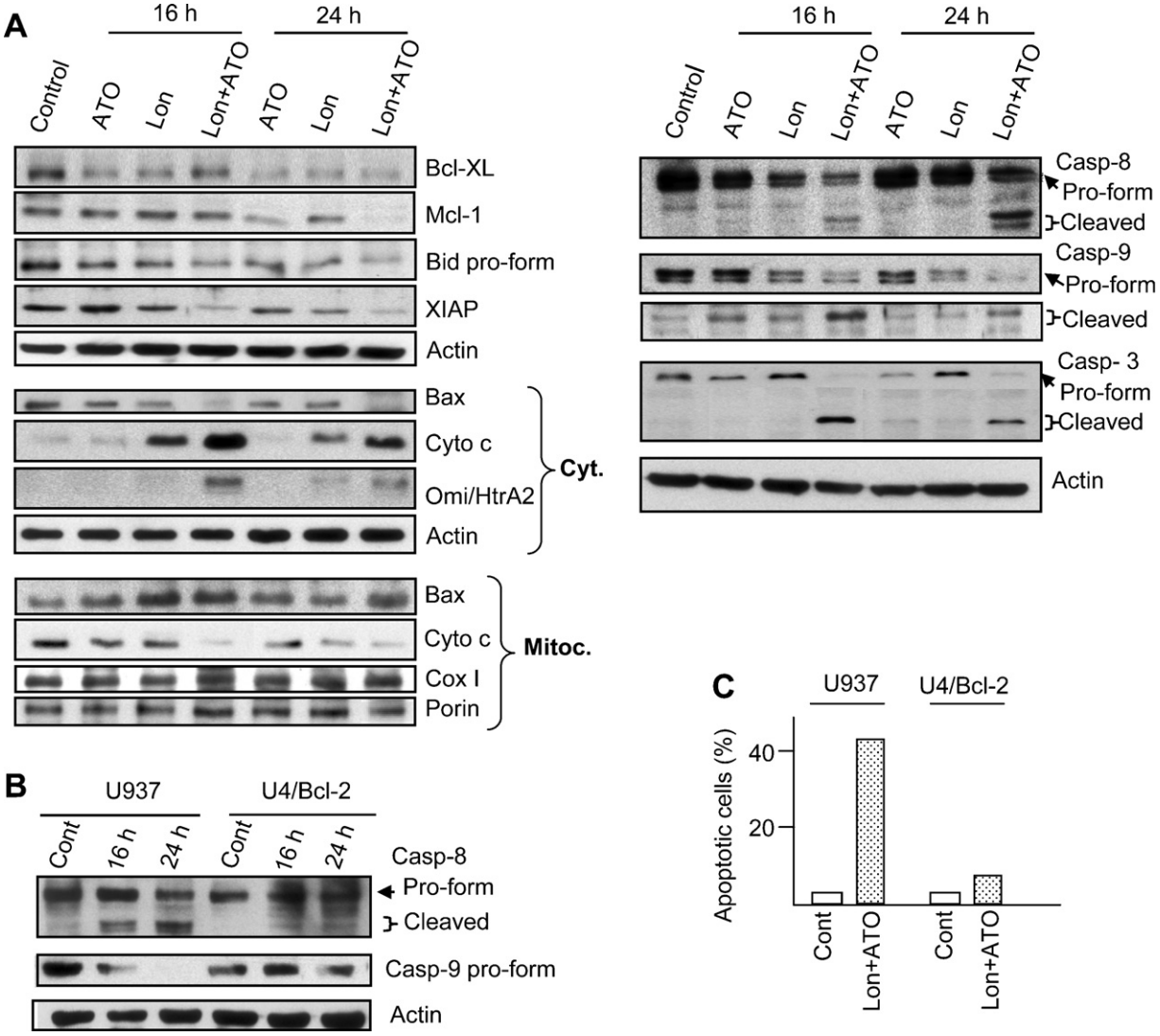

Fig. 4. Expression of apoptosis regulatory proteins. HL-60 cell cultures were treated for the indicated time periods with 100 μM lonidamine and 2 μM ATO, alone and in combination. (A) Relative levels of total Bcl-X_L, Mcl-1, Bid (23-kDa pro-form) and XIAP, as determined by immunoblot using total cellular extracts; cytochrome *c* and Omi/HtrA2 release to cytosol, and Bax remaining in cytosol, as determined using extracts from cytosolic fractions; Bax translocation to mitochondria and cytochrome *c* remaining in mitochondria, as determined using extracts from mitochondria-enriched fractions; and caspase-8, caspase-9 and caspase-3 maturation, as revealed by the decrease in pro-form intensities and the appearance of cleavage-derived fragments. Blots of caspase-9 were differently exposed since expression of cleavage fragments was very weak. The levels of β-actin were measured as a loading control in the case of total and cytosolic extracts, and the levels of COX I and VDAC/Porin in the case of mitochondria-enriched fractions. (B and C) Caspase-8 and caspase-9 (pro-form decrease) maturation (B) and apoptosis generation (C), in wild type and Bcl-2-transfected (U4/Bcl-2) U937 cells. The results in C were obtained at 24 h of treatment and represent the mean of two determinations with similar result (differences below 10%). All other conditions were as in Fig. 1.

upon treatment with lonidamine and ATO, alone and in combination. The obtained results are represented in Fig. 6. (i) Treatment with lonidamine caused a time-dependent stimulation of ERK phosphorylation, and also activated the Akt/mTOR pathway, as demonstrated by the increased phosphorylation of Akt, the mTOR-regulated p70S6K and the p70S6K-regulated rpS6. Increased ERK and Akt phosphorylation was firstly observed at hour 8, thus representing an early response in relation to apoptosis execution (see Fig. 1D) and a late event in relation to IMP generation (see Fig. 3A). Importantly, the lonidamine-provoked hyper-phosphorylation of ERK, Akt, p70S6K and rpS6 was attenuated by co-treatment with ATO. (ii) JNK phosphorylation was little affected by lonidamine or ATO alone, but was greatly stimulated by the combination of both agents. On the other hand, treatment for 8–24 h with ATO and lonidamine, alone and in combination, did not provoke relevant effects on p38-MAPK phosphorylation (result not shown), although p38-MAPK was earlier described as an oxidant-responsive kinase [27], susceptible of activation by ATO [7].

To examine the importance of kinase modulation for apoptosis, experiments were carried out using specific pharmacologic inhibitors, namely the JNK inhibitor SP600125 (20 μM), the MEK/ERK inhibitor U0126 (2.5 μM), and the phosphatidylinositol 3-kinase (PI3K) inhibitor LY294002 (30 μM). The capacity of these concentrations to prevent drug-induced kinase activation in myeloid leukemia cell models was already proved in our preceding studies [28,29]. In particular, we asked whether SP600125 could prevent lonidamine plus ATO-provoked apoptosis, and whether U0126 and/or LY294002 could mimic the pro-apoptotic action of ATO when used with lonidamine. Some of the obtained results are indicated in Fig. 7. (i) SP600125 reduced in part apoptosis generation by lonidamine plus ATO, corroborating the pro-apoptotic role of JNK (Fig. 7A). (ii) Treatments with U0126 and LY294002 separately were not toxic *per se*, and slightly increased apoptosis generation by lonidamine alone (and with more efficacy lonidamine plus ATO toxicity) (Fig. 7B). (iii) On the other hand, treatments combining U0126 plus LY294002 (a situation which

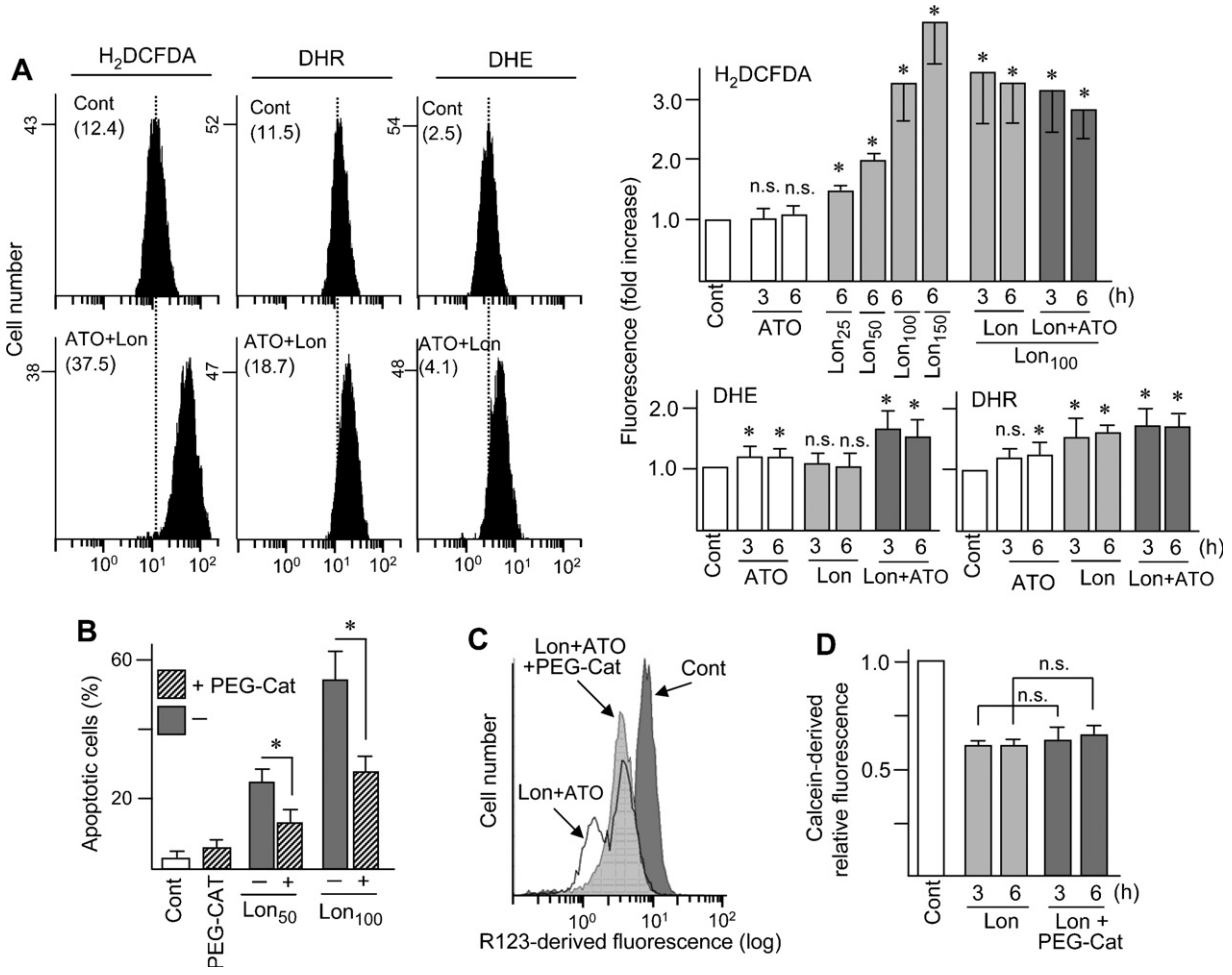

Fig. 5. ROS generation and effects of antioxidant agent. HL-60 cells were treated for 3 and 6 h (A and D) or 24 h (B and C) with 2 μM ATO and lonidamine, alone and in combination. Except when otherwise indicated, lonidamine was used at 100 μM. (A) ROS production, as measured by H_2DCFDA-, DHE- and DHR-derived fluorescence by means of flow cytometry. The cytometry profiles show examples of single determinations at 6 h with untreated (Cont) and ATO plus lonidamine-treated cells. The bar chart shows the results (mean ± SD) of at least four determinations, expressed in relation to the controls (arbitrary value of 1.0). (B–D) Apoptosis induction (B), $\Delta\Psi_m$ dissipation measured by R123 (C), and IMP production measured by calcein-AM/$CoCl_2$ (D), in the absence or the presence of PEG–Cat (1000 U/ml). The antioxidant was applied 2 h before the other agents. Note that PEG–Cat abrogates the lonidamine plus ATO-induced low-$\Delta\Psi_m$ subpopulation but not the decrease affecting the main (high-$\Delta\Psi_m$) population (C), nor the lonidamine-provoked IMP (D). Asterisks and n.s. indicate significant and non-significant differences, respectively, in relation the controls or between the indicated pair of values. All other conditions were as in Figs. 1 and 3.

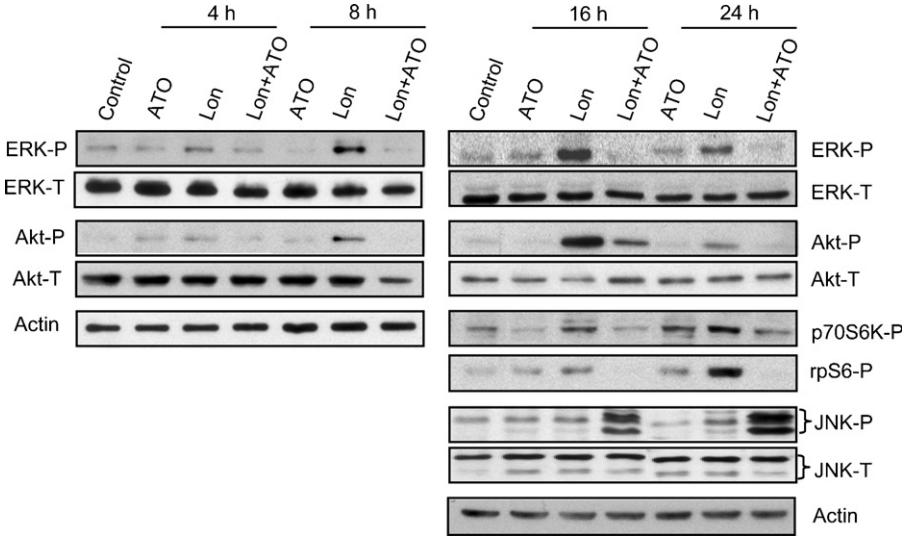

Fig. 6. Protein kinase modulation. The figure shows the relative levels of total (T) and phosphorylated (P) ERKs, Akt, p70S6K, rpS6, and JNK, in HL-60 cells treated for the indicated time-periods with 2 μM ATO and 100 μM lonidamine, alone and in combination. β-Actin was used as a loading control.

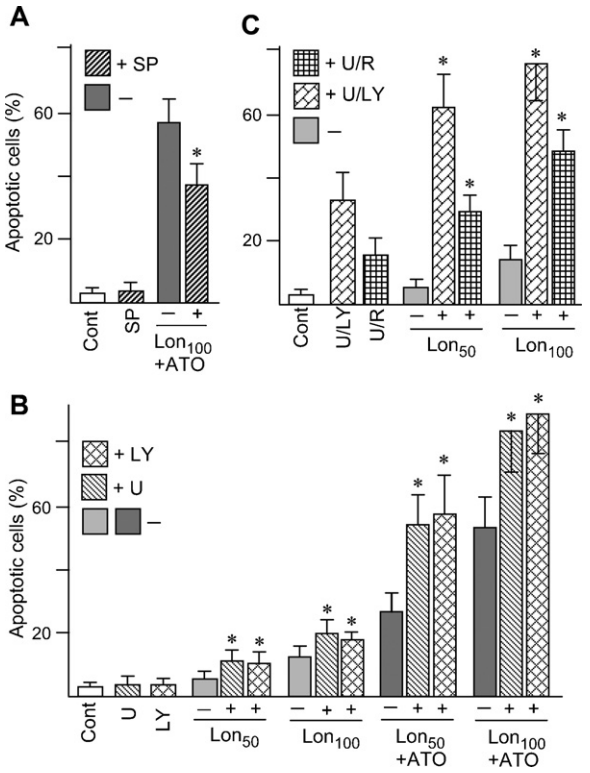

Fig. 7. Effect of protein kinase inhibitors on apoptosis induction. The figure shows the effects of (A) the JNK inhibitor SP600125 (SP), (B) the MEK/ERK inhibitor U0126 (U) and the PI3K inhibitor LY294002 (LY), and (C) the combinations of U0126 plus LY294002 or U0126 plus the mTOR inhibitor rapamycin (R), on basal, lonidamine-induced, and lonidamine plus ATO-induced apoptosis, in HL-60 cells. Determinations were carried out at 24 h of treatment using 2 μM ATO and the indicated concentrations of lonidamine, alone and in combination. SP600125 was used at 10 μM, and rapamycin at 0.1 μM. U0126 was applied at 2.5 μM when used alone, and at 0.5 μM when used together with LY294002; and LY294002 was applied at 30 μM when used alone, and at 10 μM when used together with U0126. The kinase inhibitors were applied 30 min in advance to the other agents. Asterisks in bar charts A and B indicate significant differences in relation the corresponding value without kinase inhibitor (−). Asterisks in bar chart C indicate significant differences in relation to the sum of values in individual treatments (i.e., Lon plus either U/LY or U/R). All other conditions were as in Fig. 1.

may better mimic the double inhibitory action of ATO: see Fig. 6) caused a higher increase in lonidamine-provoked apoptosis (Fig. 7C, and results not shown). Nonetheless, the simultaneous inhibition of the two survival pathways, MEK/ERK and PI3K/Akt, was already markedly toxic under basal conditions (Fig. 7C), a circumstance, which obliged us to use suboptimal inhibitor concentrations in this particular assay. Similar qualitative results were obtained using the MEK/ERK inhibitor PD98059 (20 μM, results not shown), or combining U0126 with the mTOR inhibitor rapamycin (100 nM) (Fig. 7C). Hence, allowing for the experimental limitations, these results indicate that ATO may facilitate apoptosis by preventing the lonidamine-induced activation of MEK/ERK and Akt/mTOR. Incidentally, it was reported that constitutive or drug-provoked activation of a mitochondria-located ERK pool prevents mPTP opening and subsequent apoptosis, and that this defensive response is abrogated by co-treatment with kinase inhibitor [30]. Nonetheless in our experiments treatment for 4 h with lonidamine alone or with ATO (which suffices to cause IMP) did not affect total cellular (Fig. 6) or mitochondria-associated (Supplementary Figure 3A) ERK and Akt phosphorylation, and the MEK/ERK inhibitor U0126 failed to affect lonidamine-provoked IMP (Supplementary Figure 3B). These observations seem to exclude a possible regulatory role of mitochondria-bound ERK in our experimental conditions.

4. Discussion

The results in this work indicate that lonidamine and ATO, used at clinically affordable concentrations, exhibit little apoptotic efficacy when used alone, but greatly cooperate to induce apoptosis in HL-60 and other myeloid and lymphoid human leukemia cell lines. On the other hand the combined treatment was little effective in proliferating normal PBLs, suggesting that the response was somewhat selective for tumor cells. Since both lonidamine and ATO are mitochondria-targeting drugs, we initially focused the attention on mitochondrial alterations as possible determinants for the increase in apoptosis. Lonidamine rapidly induced IMP, as revealed by the decrease in fluorescence in calcein-AM/$CoCl_2$ assays, and this represents an early response, which preceded the expression of apoptotic markers. While detailed investigation of mechanisms responsible for lonidamine-provoked IMP was beyond the purpose of this work, our preliminary observations do not sustain regulation by H_2O_2 (IMP was not inhibited by PEG–catalase) or by MEK/ERK signaling (mitochondria-bound ERK was not activated, and IMP was not potentiated by U0126) (Supplementary Figure 3), as earlier described in other experimental models [30]. We also failed to detect hexokinase 2 release from mitochondria in lonidamine- and lonidamine plus ATO-treated cells (Supplementary Figure 3), as provoked by other mitochondriotoxic agents [31]. Whatever the case, it seems clear that IMP does not adequately explain the potentiation of apoptosis in the combined treatment, since lonidamine-provoked IMP was not augmented by co-treatment with ATO. Examination of late $\Delta\Psi_m$ dissipation (which also represents an indirect manner of measuring IMP) revealed a more complex situation. As the most prominent effect, lonidamine plus ATO produced a marked $\Delta\Psi_m$ decrease affecting a discrete subpopulation, which was prevented by z-VAD-fmk and anti-oxidant (PEG–Cat) treatments, and hence likely represents the fraction of cells undergoing apoptosis. In addition, all treatments (lonidamine, ATO, and the combination) elicited a slight decrease affecting the main (high-$\Delta\Psi_m$) cell population, which was no prevented by z-VAD-fmk or the antioxidant agent. On the other hand, apoptosis potentiation by lonidamine plus ATO more clearly correlated with OMP, as revealed by the release of mitochondrial apoptogenic factors. Thus, the combined treatment exacerbated Bcl-X_L-, Mcl-1-, and Bax-regulated cytochrome *c* and Omi/HtrA2 release from mitochondria, with consequent XIAP-down-regulation and caspase-9/-3 activation. The treatment also activated the caspase-8/Bid axis which, being a Bcl-2-inhibitable response, likely represents a secondary mitochondria-dependent event. However, we may not discard the possibility that lonidamine plus ATO might directly compromise the "extrinsic" apoptotic machinery in other cell models where ATO has been reported to stimulate apoptosis mainly via death receptor-mediated pathway [32].

In addition the present results demonstrate that lonidamine induces moderate oxidative stress, as revealed by ROS over-accumulation. This result was not surprising on the ground of preceding studies, since as commented above lonidamine may inhibit the respiratory chain, which might in turn increase ROS generation. Moreover, earlier reports indicated that the expression or activity of some ANT isoforms [33,34] influence mitochondrial ROS generation. It seems clear that ROS over-production mediates at least in part apoptosis induction by lonidamine plus ATO, as demonstrated by the protective action of PEG–Cat, and with some limitations by NAC. A likely explanation is that lonidamine-provoked ROS production probably increases the intrinsic ATO toxicity, since this drug is more effective under conditions of moderate oxidative stress, as others and we demonstrated [18,22,23].

The effects of ATO on cell signaling pathways have been extensively studied, although the results are often discrepant. For instance, ATO was occasionally observed to stimulate JNK [35,36] and down-regulate ERK [35] and PI3K/Akt [36] activation in some leukemia cell models. By contrast, the effects of lonidamine on protein kinase activities and other signaling mechanism are largely unknown. As a prominent result, in this work we demonstrate that lonidamine activates ERK, Akt and mTOR (measured by the downstream substrates p70S6K and rpS6). Due to the protective action of the MEK/ERK and PI3K/Akt/mTOR pathways, we may reasonably assume that the activation of these kinases in part explains the poor apoptotic action of lonidamine when used as a single agent, and might therefore represent intervention targets to improve its limited clinical efficacy. Individual inhibition of MEK/ERK (using U0126) or PI3K/Akt (using LY294002) only slightly increased lonidamine toxicity, probably because these pathways, which are constitutively active in leukemia cells, mutually compensate. On the other hand, simultaneous down-regulation of both pathways (using U0126 plus either LY294002 or rapamycin), although already toxic under basal conditions, clearly potentiated lonidamine provoked apoptosis. On the ground of these results, we may assume that ATO potentiates lonidamine toxicity by attenuating drug-provoked activation of ERK and Akt/mTOR, and this explains in part the improved apoptotic efficacy of the lonidamine plus ATO combination. Of course, there are kinases other than ERK and Akt, which may be important for apoptosis potentiation. For instance, at the low used concentration (2 μM) ATO alone failed to elicit JNK activation, but this kinase was stimulated by lonidamine plus ATO, a response also observed when ATO was combined with other pro-oxidant agents [37]. JNK activation contributes to apoptosis potentiation, as indicated by the partial protection afforded by the JNK inhibitor SP600125. Finally, lonidamine is a glycolytic inhibitor, and our preliminary experiments indicate that lonidamine moderately decreases ATP content and stimulates the LKB1/AMPK pathway (results not shown). A detailed study of these and other signaling pathways is in progress, using different glycolytic inhibitors.

In summary, the present results indicate that combined treatment with clinically achievable concentrations of lonidamine and ATO efficaciously induce apoptosis in leukemia cell models, and hence might be useful to overcome the poor efficacy of these anti-tumor drugs when used alone. The work also elucidates some biochemical/molecular mechanisms, which may account for the cooperative effects. As prominent and totally original findings, we demonstrated that (i) lonidamine causes moderate oxidative stress, which may serve to potentiate the toxicity of ATO and perhaps other oxidant-sensitive drugs; and (ii) ATO attenuates the lonidamine-provoked activation of MEK/ERK and Akt/mTOR defensive pathways, a response which may in part account for the normally poor efficacy of lonidamine as single agent, and therefore represent important targets for pharmacologic intervention. We believe that these observations, while still representing an *in vitro* pre-clinical investigation, offers a good basis for further *in vivo* assays with potential clinical application.

Conflict of interest

The authors declare no conflict of interest.

Acknowledgements

This work was supported by the Ministerio de Ciencia e Innovación, Spain, Plan Nacional de Investigación Científica, Desarrollo e Innovación Tecnológica, Dirección General de Investigación (Grants SAF2007-64721 and SAF-2010-20256) and Programa Consolider-Ingenio 2010 (Grant CSD-00020); and by the Consejo Superior de Investigaciones Científicas (Grant 201020E037). M.C.E. is recipient of a JAE-Predoc fellowship from de Consejo Superior de Investigaciones Científicas. G.P.S. is the recipient of a "Contrato de Personal Investigador de Apoyo", Dirección General de Universidades e Investigación, Consejería de Educación, Comunidad de Madrid. The authors are very grateful to Dr. M. De las Casas (Centro de Investigaciones Biológicas, Consejo Superior de Investigaciones Científicas) for supply of freshly isolated lymphocytes.

Appendix A. Supplementary data

Supplementary data associated with this article can be found, in the online version, at Sup. doi:10.1016/j.bcp.2011.08.017.

References

[1] Di Cosimo S, Ferretti G, Papaldo P, Carlini P, Fabi A, Cognetti F. Lonidamine: efficacy and safety in clinical trials for the treatment of solid tumors. Drug Today 2003;39:157–74.
[2] Sordet O, Rébé C, Leroy I, Bruey JM, Garrido C, Miguet C, et al. Mitochondria-targeting drugs arsenic trioxide and lonidamine bypass the resistance of TPA-differentiated leukemic cells to apoptosis. Blood 2001;97:3931–40.
[3] Hulleman E, Kazemier KM, Holleman A, VanderWeele DJ, Rudin CM, Broekhuis MJ, et al. Inhibition of glycolysis modulates prednisolone resistance in acute lymphoblastic leukemia cells. Blood 2009;113:2014–21.
[4] Belzacq AS, El Hamel C, Vieira HL, Cohen I, Haouzi D, Metivier D, et al. Adenine nucleotide translocator mediates the mitochondrial membrane permeabilization induced by lonidamine, arsenite and CD437. Oncogene 2001;20:7579–87.
[5] Miller Jr WH, Schipper HM, Lee JS, Singer J, Waxman S. Mechanisms of action of arsenic trioxide. Cancer Res 2002;62:3893–903.
[6] Wang ZY, Chen Z. Acute promyelocytic leukemia: from highly fatal to highly curable. Blood 2008;11:2505–15.
[7] Platanias LC. Biological responses to arsenic trioxide. J Biol Chem 2009;284:18583–7.
[8] Amadori S, Fenaux P, Ludwig H, O'Dwyer M, Sanz M. Use of arsenic trioxide in hematologicalal malignancies: insight into clinical development of a novel agent. Curr Med Res Opin 2005;21:403–11.
[9] Renvoize R, Roger N, Moulian J, Bertoglio J, Bréard J. Bcl-2 expression in target cells leads to functional inhibition of caspase-3 protease family in human NK and lymphokine-activated killer granule-mediated apoptosis. J Immunol 1997;159:126–34.
[10] Sánchez Y, Simón GP, Calviño E, de Blas E, Aller P. Curcumin stimulates reactive oxygen species production and potentiates apoptosis induction by the antitumor drug arsenic trioxide and lonidamine in human myeloid leukemia cell lines. J Pharmacol Exp Ther 2010;335:114–23.
[11] Troyano A, Sancho P, Fernández C, de Blas E, Bernardi P, Aller P. The selection between apoptosis and necrosis is differentially regulated in hydrogen peroxide-treated and glutathione-depleted human promonocytic cells. Cell Death Differ 2003;10:889–98.
[12] Petronilli V, Miotto G, Canton M, Brini M, Colonna R, Bernardi P, et al. Transient and long-lasting openings of the mitochondrial permeability transition pore can be monitored directly in intact cells by changes in mitochondrial calcein fluorescence. Biophys J 1999;76:725–34.
[13] Poncet D, Boya P, Métivier D, Zamzami N, Kroemer G. Cytofluorometric quantitation of apoptosis-driven inner mitochondrial membrane permeabilization. Apoptosis 2003;8:521–30.
[14] Bejarano I, Redondo PC, Espino J, Rosado JA, Paredes SD, Barriga C, et al. Melatonin induces mitochondria-mediated apoptosis in HL-60 cells. J Pineal Res 2009;46:392–400.
[15] Troyano A, Fernández C, Sancho P, de Blas E, Aller P. Effect of glutathione depletion on antitumor drug toxicity (apoptosis and necrosis) in U-937 human promonocytic cells. The role of intracellular oxidation. J Biol Chem 2001;276:47107–15.
[16] Eruslanov E, Kusmartsev S. Identification of ROS using oxidized DCFDA and flow cytometry. Methods Mol Biol 2010;594:57–72.
[17] Wardman P. Fluorescent and luminescent probes for measurement of oxidative and nitrosative species in cells and tissues: progress, pitfalls, and prospects. Free Radic Biol Med 2007;43:995–1022.
[18] Sánchez Y, Amrán D, Fernández C, de Blas E, Aller P. Genistein selectively potentiates arsenic trioxide-induced apoptosis in human leukemia cells via oxygen species generation and activation of reactive oxygen species-inducible protein kinases (p38-MAPK, AMPK). Int J Cancer 2008;123:1205–14.
[19] Galán A, García-Bermejo ML, Troyano A, Vilaboa NE, de Blas E, Kazanietz MG, et al. Stimulation of p38 mitogen-activated protein kinase is an early regulatory event for the cadmium-induced apoptosis in human promonocytic cells. J Biol Chem 2000;275:11418–24.
[20] Zunino SJ, Storms DH. Resveratrol-induced apoptosis is enhanced in acute lymphoblastic leukemia cells by modulation of the mitochondrial permeability transition pore. Cancer Lett 2006;240:123–34.

[21] Fulda S, Debatin KM. Extrinsic versus intrinsic apoptosis pathways in anticancer chemotherapy. Oncogene 2006;25:4798–811.
[22] Yi J, Gao F, Shi G, Li H, Wang Z, Shi X, et al. The inherent cellular level of reactive oxygen species: one of the mechanisms determining apoptotic susceptibility of leukemic cells to arsenic trioxide. Apoptosis 2002;7:209–15.
[23] Pelicano H, Feng L, Zhou Y, Carew JS, Hileman EO, Plunkett W, et al. Inhibition of mitochondrial respiration: a novel strategy to enhance drug-induced apoptosis in human leukemia cells by reactive oxygen species-mediated mechanism. J Biol Chem 2003;39:37832–9.
[24] Floridi A, Lehninger AL. Action of the antitumor and antispermatogenic agent lonidamine on electron transport in Ehrlich ascites tumor mitochondria. Arch Biochem Biophys 1983;226:73–83.
[25] Wada T, Penninger JM. Mitogen-activated protein kinases in apoptosis regulation. Oncogene 2004;23:2838–49.
[26] Tabellini G, Cappellini A, Tazzari PL, Falà F, Billi AM, Manzoli L, et al. Phosphoinositide 3-kinase/Akt involvement in arsenic trioxide resistance in human leukemia cells. J Cell Physiol 2005;202:623–34.
[27] Kurata S. Selective activation of p38 MAPK cascade and mitotic arrest caused by low level oxidative stress. J Biol Chem 2000;275:23413–6.
[28] Fernández C, Ramos AM, Sancho P, Amrán D, de Blas E, Aller P. 12-O-Tetradecanoylphorbol-13-acetate may both potentiate and decrease the generation of apoptosis by the antileukemic agent arsenic trioxide in human promonocytic cells. Regulation by extracellular signal-regulated protein kinases and glutathione. J Biol Chem 2004;279:3877–84.
[29] Ramos AM, Fernández C, Amrán D, Sancho P, de Blas E, Aller P. Pharmacologic inhibitors of PI3K/Akt potentiate the apoptotic action of the antileukemic drug arsenic trioxide via glutathione depletion and increased peroxide accumulation in myeloid leukemia cells. Blood 2005;105:4013–20.
[30] Rasola A, Sciacovelly M, Chiara F, Pantic B, Brusilov WS, Bernardi P. Activation of mitochondrial ERK protects cancer cells from death through inhibition of the permeability transition. Proc Natl Acad Sci USA 2010;107:726–31.
[31] Mathupala SP, Ko YK, Pedersen PL. Hexokinase 2 bound to mitochondria: cancer's sygian link to the "Warburg effect" and a pivotal target for effective therapy. Semin Cancer Biol 2009;19:17–24.
[32] Akay C, Gazitt Y. Arsenic trioxide selectively induces early and extensive apoptosis via APO2/caspase-8 pathway engaging the mitochondrial pathway in myeloma cells with mutant p53. Cell Cycle 2003;2:358–68.
[33] Le Bras M, Borgne-Sanchez A, Touat Z, El Dein OS, Deniaud A, Maillier E, et al. Chemosensitization by knockdown of adenine nucleotide translocase-2. Cancer Res 2006;66:9143–52.
[34] Gallerne C, Touat Z, Chen ZX, Martel C, Mayola E, Sharaf El Dein OS, et al. The four isoform of the adenine nucleotide translocator inhibits mitochondrial apoptosis in cancer cells. Int J Biochem Cell Biol 2010;42:623–9.
[35] Shim MJ, Kim HJ, Yang SJ, Lee IS, Choi HI, Kim T. Arsenic trioxide induces apoptosis in chronic myelogenous leukemia K562 cells: possible involvement of p38 MAP kinase. J Biochem Mol Biol 2002;35:377–83.
[36] Redondo-Muñoz J, Escobar-Díaz E, Hernández Del Cerro M, Padiella A, Terol MJ, García-Marco JA, et al. Induction of B-chronic lymphocytic leukemia cell apoptosis by arsenic trioxide involves suppression of the PI3K/Akt survival pathway via c-jun-NH2 terminal kinase activation and PTEN up regulation. Clin Cancer Res 2010;16:4382–91.
[37] Chen D, Chan R, Waxman S, Jing Y. Buthionine sulfoximine enhancement of arsenic trioxide-induced apoptosis in leukemia and lymphoma cells is mediated via activation of c-Jun NH2-terminal kinase and up-regulation of death receptors. Cancer Res 2006;66:11416–23.